JOURNAL OF OPTOELECTRONICS AND ADVANCED MATERIALS, Vol. 11, No. 8, August 2009, p. 1178 - 1184

Dynamics analysis and fuzzy logic controller design of atomic force microscope system with uncertainties

HER-TERNG YAU[a*] , CHENG-CHI WANG[b]
[a]*Department of Electrical Engineering, Far-East University, No 49, Jung-Hwa Road, Hsin-Shih Town Tainan 744, Taiwan, R.O.C*
[b]*Department of Mechanical Engineering, Far-East University, No 49, Jung-Hwa Road, Hsin-Shih Town Tainan 744, Taiwan, R.O.C.*

In this paper a nonlinear rule based fuzzy logic controller is proposed to control the nonlinear dynamic behavior of the probe tip of an atomic force microscope system (AFMs). At first, we use the bifurcation diagram to analysis the complex dynamic behavior of the atomic force microscope system, and show that the chaotic behaviour exists in the region of $A_3 > 2.54$. Next, in order to suppress the undesired motion in AFMs with uncertainty, we address the design schemes of fuzzy logic controller to stabilize the slave AFMs with parameter uncertainty to the master AFMs. Based on Lyapunov stability theory and fuzzy rules, the nonlinear controller and some generic sufficient conditions for global asymptotic synchronization are attained. We directly construct the fuzzy rules subject to a common Lyapunov function such that the error dynamics of master and slave AFMs satisfy stability in the Lyapunov sense. It overcomes the trial-and-error tuning for the membership functions and rule base in traditional fuzzy logic control. The effectiveness of presented method is numerically investigated by synchronizing slave AFMs which has chaotic motion or exceeding vibration amplitude to the master AFMs which is periodic motion or has small vibration amplitude.

(Received April 15, 2009; accepted July 29, 2009)

Keywords: AFMs, Microcantilevers, Chaotic motion, Fuzzy controller

1. Introduction

Atomic force microscope (AFM) provides a powerful tool for surface analysis applications in the nano-electronics, materials and biotechnology fields. The mechanism of AFM basically depends on the interaction of a microcantilever with surface forces. The tip of the microcantilever interacts with surface through a surface–tip interaction potential. One approach to measure the surface forces is to monitor the deflection of the microcantilever through a photodiode. This approach is named “contact mode”. Another approach termed “tapping mode”, is performed by vibrating the microcantilever close to its resonance frequency and monitoring the changes in its effective spring constant. In this method, the driving amplitude is set to a constant value and typical resonant frequencies are in the range from a few kilohertz to some megahertz [2].

The nonlinear dynamic behavior of an AFM system is a major concern since any irregular motion of the AFM probe tip inevitably degrades the precision of the measurement results. Burnham et al. [1-2] showed that the microcantilever of an AFM performed chaotic motion under specific physical conditions. Ashhab et al. [3] modeled the microcantilever of an AFM using a single-frequency mode approximation and analyzed the chaotic dynamics of the cantilever-sample system using the Melnikov method. Lee et al. [4] analyzed the effects of van der Waals and Derjaguin-Muller-Toporov forces on the tip-sample interactions induced in dynamic force microscopy (DFM). The authors also presented detailed experimental results which provided valuable new perspectives and insights into DFM. Ruetzel et al. [5] applied the Galerkin method to investigate the nonlinear dynamics of an AFM probe tip under the assumption that the tip-surface interactions were governed by Lennard-Jones potentials. Based upon their analysis, the authors showed that a microcantilever in tapping mode exhibited a broad range of dynamic phenomena, including both periodic and chaotic motion.

The existence of chaotic motion in AFMs is highly undesirable for its performance since this type of complex irregular motion causes the AFM to give inaccurate measurements and low resolution of the achieved sample topography. Accordingly, it is always required to ensure good performance of the microscope and to eliminate the possibility of chaotic motion of the microcantilever either by changing the AFM operating conditions to a region of the parameter space where regular motion is enssured or by designing an active controller to remove the chaotic motion.. In 1999, Ashhab et al.[6] applied a proportional and derivative controller to AFMs, firstly. It computes the Melnikov function in terms of the parameters of the controller. Using this relation it is possible to design controllers that will remove the possibility of chaos in AFMs. Besides, In 2008, Arjmand et al. [7] used a nonlinear delayed feedback control to control chaos in AFMs. It showed that the chaotic behaviour of the AFMs is suppressed by stabilizing one of its first-order Unstable Periodic Orbits via sliding mode control.

Many methods have been presented for the control and synchronization of chaotic system [8-11]. However, none of the studies reviewed above presented a fuzzy controller to remove the chaotic motion in AFMs. Accordingly, the present study investigates the dynamic behavior of an AFM probe tip in tapping mode by reference to bifurcation diagrams and phase portraits of the tip displacement and tip velocity. Otherwise, Poincaré maps and maximum Lyapunov exponent are used to identify the onset of chaotic behavior in the AFMs system. In order to remove the chaotic motion or eliminate the exceeding vibration amplitude in AFMs, a controller with a set of fuzzy rules is designed for synchronizing the slave AFMs which included undesired behaviour to the master AFMs which is periodic motion or has small vibration amplitude. To overcome the trail-and-error tuning of the membership functions and rule base, we directly construct the fuzzy rules subject to a common Lyapunov function such that the error dynamics satisfies stability in the Lyapunov sense. Simulation results show that the proposed controller drives the slave AFMs to synchronize to the master AFMs.

The remainder of this paper is organized as follows. Section 2 presents a system description for the time-dependent motions of the microcantilever tip. Section 3 describes the fuzzy logic controller design procedure in AFMs. Numerical simulations that confirm the validity and feasibility of the proposed method are shown in section 4. Finally, Section 5 draws some brief conclusions.

2. Mathematical modelling

The behavior of an AFM probe tip in which the tip-surface interactions are governed by the Lennard-Jones potential function can be modeled using the following non-dimensional single-degree-of-freedom model: [5]

$$\dot{x}_1 = x_2 \tag{1}$$

$$\dot{x}_2 = -x_1 + \frac{A_1}{(z - x_1)^2} - \frac{A_1 A_2{}^6}{30(z - x_1)^8} + A_3 \sin \Omega t + A_3 A_4 \Omega \cos \Omega t - A_4 x_2 \tag{2}$$

In the above expression, t is the non-dimensional time, x_1 indicates the non-dimensionalized displacement of the microcantilever tip (where a positive value indicates a displacement towards the sample), x_2 denotes the non-dimensionalized microcantilever tip velocity of the microcantilever, and z is the vibrational amplitude of the dither piezoelectric actuator which drives the tip. Note that both x_1 and z are non-dimensionalized by the gap between the tip and the sample under equilibrium conditions. In the case where the excitation frequency is close to the natural frequency of the microcantilever, Ω=1. Furthermore, assuming a Si-Si probe-sample system, the coefficients in Eq. (2) have the following values: z=2.0, A1 = 4/27, A2 =0.3, A4= 0.03 and A3 is from 0.1 to 3.0. The bifurcation diagrams of x_1 and x_2 are shown in Fig.1 (a) and 1(b), respectively. It shown that the system state exist complex dynamics. From local bifurcation diagram (Fig. 2), it can be seen that the dynamics of AFMs will change from periodic motion to aperiodic motion after the parameter A_3 is greater than 2.54. The phase plane trajectories of periodic motions with $A_3 = 2.1$ (period T) and $A_3 = 2.2$ (period 2T), and aperiodic motion with $A_3 = 2.6$ are shown in Fig. (3). From Fig. (4), it can be seen that in the Poincaré map exists a strange attractor, and a positive maximum Lyapunov exponent is obtained at $A_3 = 2.6$. Therefore, it guarantees that the AFMs fell into chaotic motion at this condition.

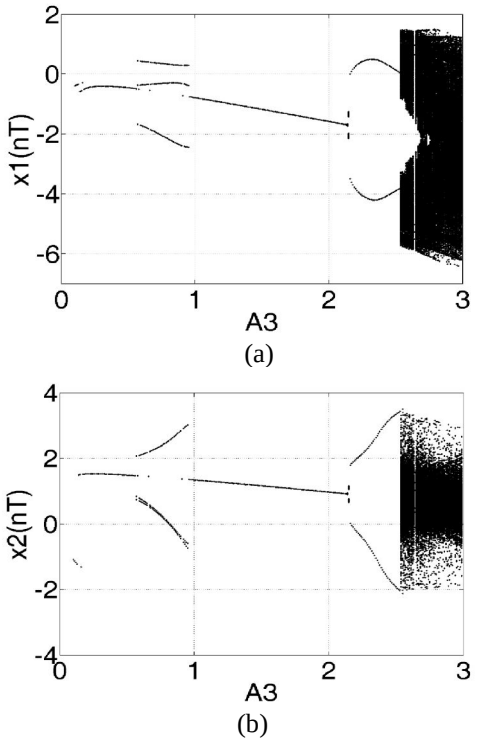

Fig. 1. Bifurcation diagrams versus A_3: (a) x1(nT) and (b) x2(nT).

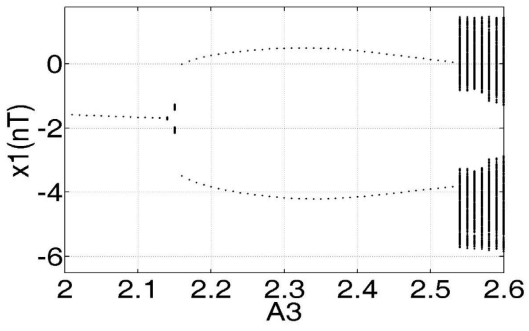

Fig. 2. Local bifurcation diagram of x1(nT) versus A_3.

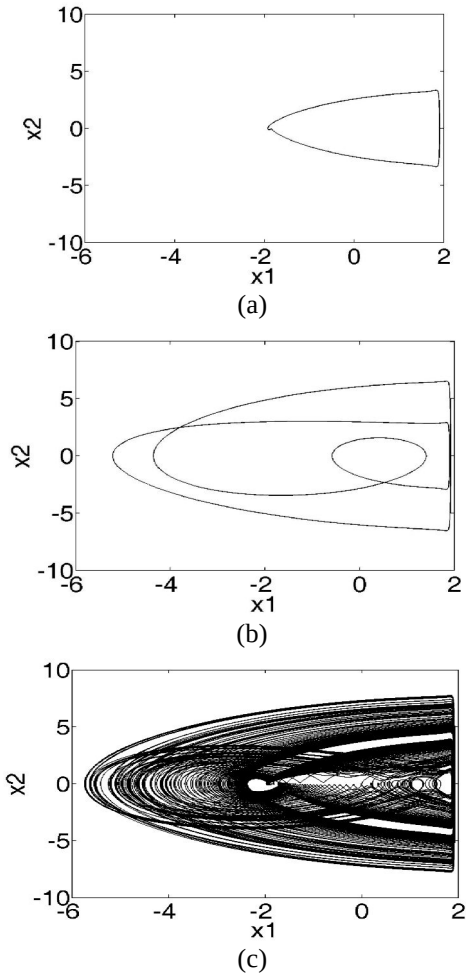

Fig. 3. The steady sate trajectories of AFMs ; (a) $A_3 = 2.1$ *, (b)* $A_3 = 2.5$ *, (c)* $A_3 = 2.6$

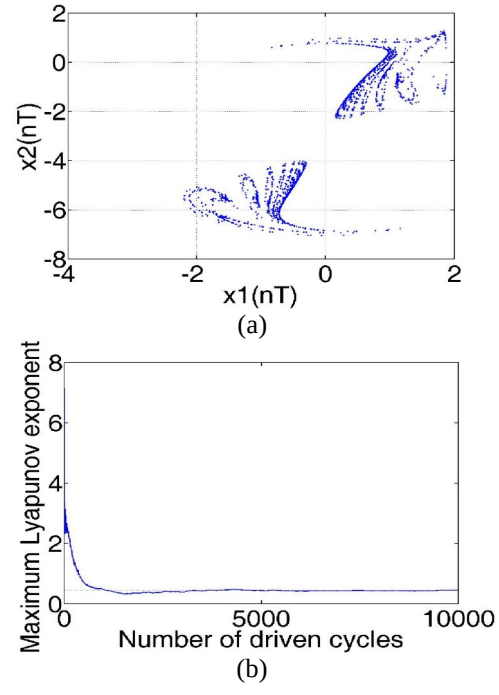

Fig. 4. The strange attractor (a) and maximum Lyapunov exponent (b) of chaotic motion with $A_3 = 2.6$.

Consider two AFMs as follows

Master system:

$$\begin{cases} \dot{x}_1 = x_2 \\ \dot{x}_2 = -x_1 + \dfrac{A_1}{(z - x_1)^2} - \dfrac{A_1 A_2{}^6}{30(z - x_1)^8} \\ \qquad + A_3 \sin \Omega t + A_3 A_4 \Omega \cos \Omega t - A_4 x_2 \end{cases}, \tag{3}$$

Slave system:

$$\begin{cases} \dot{y}_1 = y_2 \\ \dot{y}_2 = -y_1 + \dfrac{A_1}{(z - y_1)^2} - \dfrac{A_1 A_2{}^6}{30(z - y_1)^8} + (A_3 + \Delta A_3) \cdot \sin \Omega t \\ \qquad + (A_3 + \Delta A_3) \cdot A_4 \Omega \cos \Omega t - A_4 y_2 + u(t) \end{cases}, \tag{4}$$

where $u \in R$ is the control input. The master AFMs is a periodic motion and has good performance of the microscope in this study. ΔA_3 is an uncertain term or structural variation of A_3 . It may cause the original slave AFMs which is identical to the master AFMs to generate a great change such as from periodic motion to aperiodic motion or from period T to period 2T. Beside, ΔA_3 also can to increase the vibration amplitude of the micro-cantilever of AFMs. Therefore, the ΔA_3 may cause the undesired behavior in AFMs for its bad effects on the system since it will lead the AFMs to give inaccurate measurements and low resolution of the achieved sample topography. The control input $u(t)$ attached in slave AFMs will synchronize the slave system to master system, that is

$$\lim_{t \to \infty} \| x(t) - y(t) \| \to 0 , \tag{5}$$

where $\| \cdot \|$ is the Euclidean norm of a vector. This scheme can be used in the real AFM operation when the undesired motion comes into being.

3. Fuzzy controller design

The aim of this study is to apply the fuzzy logic control to AFMs. Fuzzy logic has come a long way since it was first presented to technical society, when Zadeh [12] published his seminal work “Fuzzy Sets” in the Journal of Information and Control. Since that time, the subject has been the focus of much independent research. The attention currently being paid to fuzzy logic is most likely the result of present popular consumer products employing fuzzy logic [13]. The superior qualities of this method include its simplicity, satisfactory performance and robust character. However, it takes a long time to obtain the membership functions and rule base by trial-and-error tuning in traditional FLC design. To overcome the trail-and-error tuning of the membership functions and rule base, we directly construct the fuzzy rules subject to a common Lyapunov function such that the error dynamics satisfies stability in the Lyapunov sense. The basic configuration of

the fuzzy logic system is shown in Fig. 5.

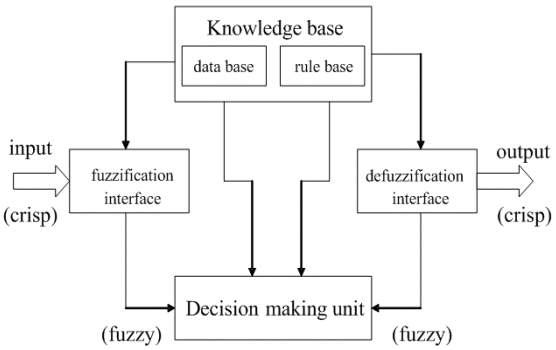

Fig. 5. The configuration of fuzzy logic controller.

For the synchronization systems (3) and (4), let the error states are $e_1 = y_1 - x_1$ and $e_2 = y_2 - x_2$. Subtracting (3) from (4) yields the synchronization error dynamics as

$$\begin{cases} \dot{e}_1 = e_2 \\ \dot{e}_2 = -e_1 - A_4 e_2 + f(x_1, y_1) + g(t) + u(t) \end{cases}, \tag{6}$$

where

$$f(x_1, y_1) = A_1\left[\frac{1}{(z-y_1)^2} - \frac{1}{(z-x_1)^2}\right] - \frac{A_1 A_2^6}{30}\left[\frac{1}{(z-y_1)^8} - \frac{1}{(z-x_1)^8}\right],$$

and

$\Delta g(t) = \Delta A_3 \cdot \sin \Omega t + \Delta A_3 \cdot A_4 \Omega \cos \Omega t$.

Let the control input $u(t) = u_{eq} + u_L$ and $u_{eq} = -f(x_1, y_1)$, then the error dynamics becomes

$$\begin{cases} \dot{e}_1 = e_2 \\ \dot{e}_2 = -e_1 - A_4 e_2 + \Delta g(t) + u_L \end{cases} \tag{7}$$

Where, $\Delta g(t)$ is the small system uncertainty of external excitation term for the base in the AFMs. In the real physical AFMs, it can be assumed to be bounded, that is $|\Delta g(t)| \le \alpha$.

In this study, Matlab Simulink with Fuzzy Toolbox is used. The aim of the fuzzy logic control system for the AFMs uses the errors (e_1, e_2) as the antecedent part of the proposed FLC to design the control input u_L that will be used in the consequent part of the proposed FLC i.e.:

$$u_L = FLC(e_1, e_2), \tag{8}$$

where the FLC accomplishes the objective to stabilize the error dynamics (7).

Table 1 lists the fuzzy rule base in which the input variables in the antecedent part of the rules are e_1 and e_2, and the output variable in the consequent is u_{Li}. Using P, Z and N as input fuzzy sets representing 'postive', 'zero' and 'negative', respectively, we obtain the membership function shown in Fig. 6. The combination of the two input variables (e_1, e_2) forms n=9 heuristic rules in Table 1 and each rules belongs to one of the three fuzzy sets P, Z and N. The first rule in Table 1 is given as:

IF e_1 is P and e_2 is P THEN output is u_{L1}.

All the rules are written using Mamdani method to apply to fuzzification in Fig. 6.

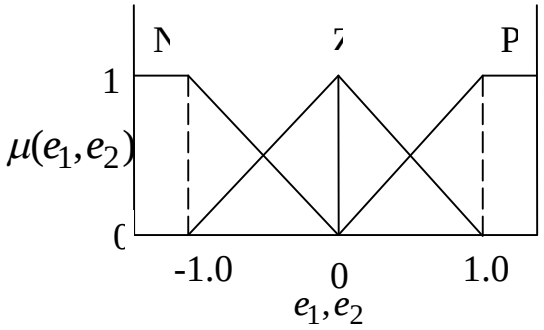

Fig .6. Membership functions.

In this study, the centroid method is used in defuzzification.

From system (7), we select a Lyapunov function such that:

$$V = \frac{1}{2}(e_1^2 + e_2^2), \tag{9}$$

which is obviously positive and continuously differentiable. The corresponding requirement of Lyapunov stability [21] is

$$\dot{V} = e_1\dot{e}_1 + e_2\dot{e}_2 < 0, \text{ that is } \dot{e}_2 < -\frac{e_1\dot{e}_1}{e_2}. \tag{10}$$

According the Lyapunov stability condition (10), the following case will satisfy all the stability conditions.

Case1: $e_2 < 0$

For $e_2 < 0$, the Eq.(10) becomes to

$$\dot{e}_2 > -e_1. \tag{11}$$

Substituting Eq.(11) into Eq.(7) yields

$-e_1 - A_4 e_2 + \Delta g(t) + u_L > -e_1$,

hence $u_L > A_4 e_2 - \Delta g(t)$. We can define that

$$A_4 e_2 + \alpha = u_1^*. \tag{12}$$

Case2: $e_2 > 0$

For $e_2 > 0$, the Eq.(10) becomes to

$$\dot{e}_2 < -e_1 \tag{13}$$

Substituting Eq.(13) into Eq.(7) yields

$$\dot{e}_2 = -e_1 - A_4 e_2 + \Delta g(t) + u_L < -e_1, \quad (14)$$

hence $u_L < A_4 e_2 - \Delta g(t)$. It is defined that

$$A_4 e_2 - \alpha = u_2^*. \quad (15)$$

If the system satisfies the case1 and case 2, then $\dot{V} < 0$ and the error state will be asymptotically driven into zero. In order to achieve this result, we will design u_L by rule table in the next work in this paper.

According to the stability analysis method [8], only those fuzzy subsystems that corresponding to each rule need to be considered. From table 1, it can be seen that e_1, e_2 are belong to fuzzy sets P, Z and N . The heuristic rules in Table 1 are divided into five parts to discuss the stability of each subsystem. For rules 1, 4 and 7 in table 1, the error state e_2 is positive, and $\dot{e}_2 < -e_1$ and $u_{L1} = u_{L4} = u_{L7} = u_2^*$. The corresponding derivative of the Lyapunov function in (10) is

$$\dot{V} = e_1 \dot{e}_1 + e_2 \dot{e}_2 = e_2 (e_1 + \dot{e}_2) < 0. \quad (16)$$

Similarly, for rules 3, 6 and 9 in table 1, the error state e_2 is negative, and $\dot{e}_2 > -e_1$ and $u_{L3} = u_{L6} = u_{L9} = u_1^*$. The corresponding derivative of the Lyapunov function in (9) also satisfies $\dot{V} < 0$.

Case3: $e_1 > 0$ and $e_2 \in$ zero

For rule 2 in table 1, the error state e_1 is positive and e_2 is zero. If the corresponding derivative of the Lyapunov function needs to be still kept negative in (10), then it needs to be satisfied

$$e_1 + \dot{e}_2 = -\mathrm{sgn}(e_2), \quad (17)$$

where $\mathrm{sgn}(e_2) = \begin{cases} 1; e_2 > 0 \\ -1; e_2 < 0 \end{cases}$.

Because of e_1 is positive, then

$$\dot{e}_2 < -\mathrm{sgn}(e_2). \quad (18)$$

Substituting equation (18) into equation(7) yields

$$-e_1 - A_4 e_2 + \Delta g(t) + u_L < -\mathrm{sgn}(e_2). \quad (19)$$

The above equation can be rewritten as

$$u_L < -\mathrm{sgn}(e_2) + e_1 + A_4 e_2 - \Delta g(t), \quad (20)$$

and it is defined that

$$u_{L2} = -\mathrm{sgn}(e_2) + e_1 + A_4 e_2 - \alpha. \quad (21)$$

Case4: $e_1 < 0$ and $e_2 \in$ zero

The controller u_{L8} in rule 8 will be discussed similarly to rule 2 in table 1. Because of e_1 is negative then

$$\dot{e}_2 > -\mathrm{sgn}(e_2). \quad (22)$$

Substituting equation(22) into equation(7) yields

$$-e_1 - A_4 e_2 + \Delta g(t) + u_L > -\mathrm{sgn}(e_2). \quad (23)$$

The above equation can be rewritten as

$$u_L > -\mathrm{sgn}(e_2) + e_1 + A_4 e_2 - \Delta g(t), \quad (24)$$

and it is defined that

$$u_{L2} = -\mathrm{sgn}(e_2) + e_1 + A_4 e_2 + \alpha. \quad (25)$$

Case5: $e_1 \in$ zero and $e_2 \in$ zero

For rule 5 in table 1, the error states e_1 and e_2 is zeros. This condition is included in the other rules, and we define $u_L = u_{L5} = 0$ in this rule.

Hence, all of the rules in the FLC can lead to Lyapunov stable subsystems under the same Lyapunov function (9). Furthermore, the closed-loop rule-based system (6) and (7) are asymptotically stable for each derivate of the Lyapunov function that satisfies $\dot{V} < 0$ in Table 1. That is, the states (e_1, e_2) guarantee convergence to zero and the two nonlinear master-slave AFMs is synchronized.

4. Results and discussion

In this section, some numerical experiments are presented to demonstrate and verify the performance of the present design. The 5th order Runge-Kutta algorithm was used to obtain the numerical solutions of systems (3) and (4) with a time grid of 0.001. For the overall control systems (3) and (4), the parameters are A1 = 4/27, A2 =0.3, $\Delta A_3 = 0.1$, A4= 0.03, $\Omega = 1$, $z = 2$, and the initial conditions are $x_1(0)=0$, $x_2(0)=0$, $y_1(0)=0$, $y_2(0)=0$.

In the first case, the A3 is 2.1. From Fig. 2, it can be seen that the master system (3) is in a state of periodic motion with period T at this condition. However the slave system will be perturbed to another periodic motion with period 2T and generated undesired larger vibration amplitude by the uncertainty term ΔA_3 under control input $u = 0$. In Figs. 7-8, it shows that the slave system with period 2T will be synchronized to the master system with period T by FLC after the controller is active at $t = 1500$. In addition, the phase plane trajectories of controlled slave system and the error states are shown in Figs. 9-10. It can be seen that the system error states are regulated to zeros asymptotically.

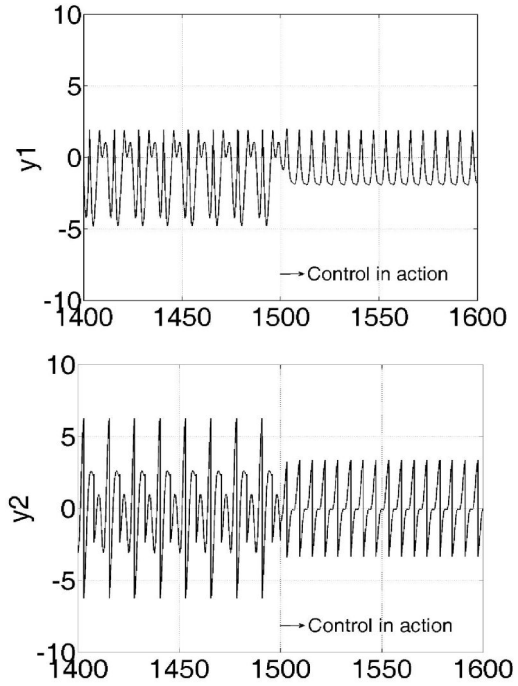

Fig. 7. The time history of controlled periodic master (x1, x2) and chaotic slave (y1, y2) systems: (a) x1, y1 versus t; (b) x2, y2 versus t. The controller is active from t=1500.

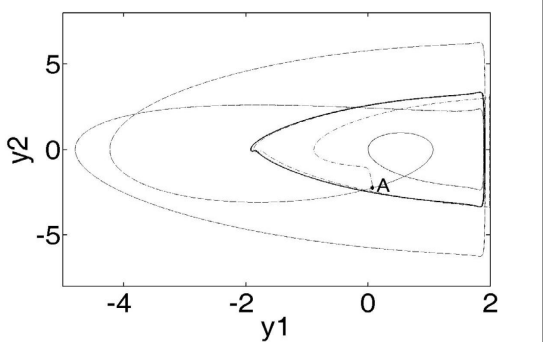

Fig. 8. The controlled phase plane trajectory of slave system. The dashed line is period 2T and solid line is period T, and the controller is active from point A (t=1500).

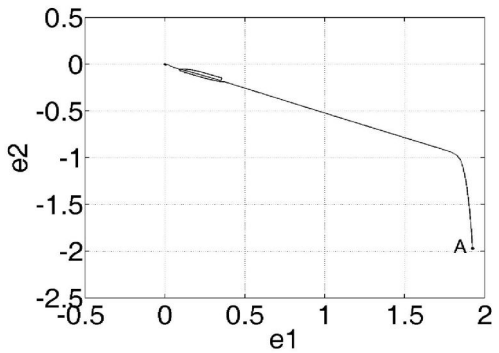

Fig. 9. The error state trajectories in phase plane trajectory of master-slave AFM system; the controller is active from point A (t=1500).

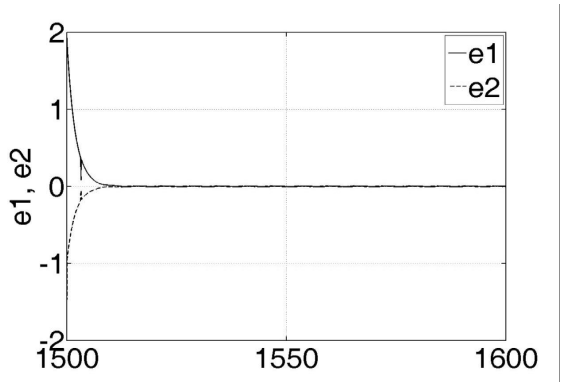

Fig. 10. The time responses of synchronization error.

In the second case, the A_3 is 2.5. Fig. 2, shows that the master system (3) is in a state of periodic motion with period 2T at this condition. However the slave system will be perturbed to chaotic motion by the uncertainty term ΔA_3 under control input $u = 0$. Figs. 11-14, show that the slave system with chaotic behavior will be synchronized to the periodic master system with period 2T by FLC after the controller is active at $t = 1500$.

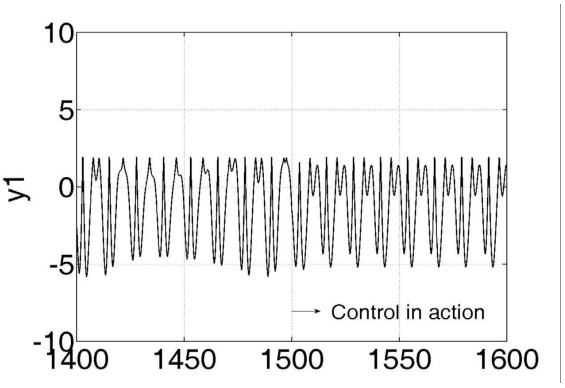

a

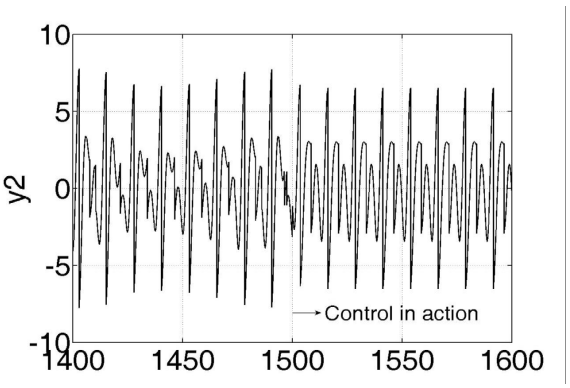

b

Fig. 11. The time history of controlled periodic master (x1, x2) and chaotic slave (y1, y2) systems: (a) x1, y1 versus t ; (b) x2, y2 versus t. The controller is active from t=1500.

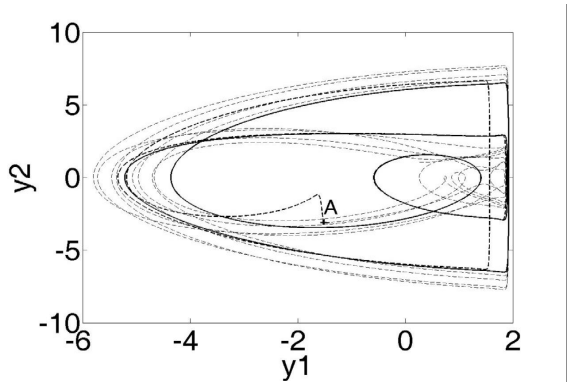

Fig. 12. The controlled phase plane trajectory of slave system. The dashed line is chaotic motion and solid line is period 2T, and the controller is active from point A (t=1500).

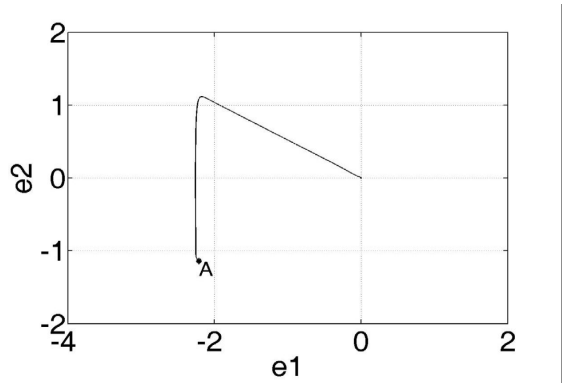

Fig. 13. The error state trajectories in phase plane trajectory of master-slave AFM system; the controller is active from point A (t=1500).

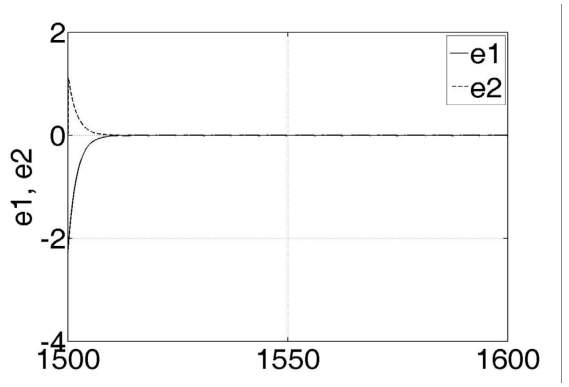

Fig. 14. The time responses of synchronization error.

5. Conclusions

In this study, the dynamic analysis and fuzzy logic synchronization control with parameter uncertainty for AFMs have been demonstrated. The main idea behind the proposed fuzzy logic controller is the great potential in active control in AFMs. Since the chaotic motion and enormous vibration amplitude are undesired in AFMs, the FLC is used to synchronize the slave system with undesired behavior to the master system with suitable behavior. The simulation results show that the implementation of fuzzy logic controller offers a good response as far as removing the undesired behavior in AFMs. Simulations results show that the proposed controllers have a satisfactory performance.

Acknowledgements

The financial support of this research by the National Science Council of the R.O.C., under Grant No. 96-2221-E-269-010-MY2 is greatly appreciated.

References

[1] N. A. Burnham, R. J. Colton, H. M. Pollock, Nanotechnology, **4**, 64 (1993).
[2] N. A. Burnham, A. J. Kulik, G. Germaud, G. A. D. Briggs, Phys. Rev. Lett. **74**, 5092 (1995).
[3] M. Ashhab, M.V. Salapaka, M. Dahleh, I. Mezic, Nonlinear Dyn. **20**, 197 (1999).
[4] S. I. Lee, S. W. Howell, A. Raman, R. Reifenberger, Ultramicroscopy **97**(1-4), 185 (2003).
[5] S. Ruetzel, S.I. Lee, A. Raman, Proc. R. Soc. London A, **459**,1925 (2003).
[6] M. Ashhab, M. V. Salapaka, M. Dahleh, I. Mezic, Automatica **35**, 1663 (1999).
[7] M. T. Arjmand, H. Sadeghian, H. Salarieh, A. Alasty, Nonlinear Analysis: Hybrid Systems **2**, 993 (2008).
[8] G. Chen, X. Dong, From chaos to order: methodologies, perspectives and applications. Singapore: World Scientific, (1998).
[9] H.T. Yau, Mechanical Systems and Signal Processing. **22**, 408 (2008).
[10] H. T. Yau, C. L. Kuo, J. J. Yan , International Journal of Nonlinear Sciences and Numerical simulation **7**(2), 333 (2006).
[11] S. Oancea, J. Optoelectron. Adv. Mater. **7**(6), 2919 (2005).
[12] L. Zadeh, Journal of Information and Control **8**, 338 (1965).
[13] T. J. Ross, Fuzzy Logic with Engineering Applications, McGraw-Hill Inc, New York, (1995).

*Corresponding author: pan1012@ms52.hinet.net